



ZERO GRAVITY—Dr. Vemuri Balakotaiah, professor of chemical engineering (*l.*), and Dr. Dmitri Lastochkin, post-doctoral fellow (*r.*), engage in laboratory experiments that led to seven sets of experiments aboard the KC-135 aircraft. In zero-gravity flight, they study the characteristics of wavy films in gas-liquid flows in the viscous regime to measure slug-annular transition points and pressure drop in microgravity.

Experimental and Modeling Studies on Wavy Films in Annular Gas-Liquid Two-Phase Flows under Normal and Microgravity Conditions

10-ISSO

Abstract—

Experiments have been conducted under both normal and microgravity conditions to determine the characteristics of wavy films in annular gas-liquid two-phase flows in pipes. In normal gravity experiments in a vertical pipe, researchers observed a new phenomenon of wave suppression at moderately high Reynolds numbers. They found that the maximum as well as the average wave amplitudes reach a maximum value at some Reynolds number and then start to decrease. This observation is contrary to the well-established point of view that wave amplitude increases with the Reynolds number. In some experiments, completely flat films were observed with Reynolds numbers in the range 300-1400. The suppression of waves on vertically falling films was observed only in a window of fluid viscosities of 0.005 to 0.025 Pa.s for the case of pipe with an internal diameter of 1.27 cm. For viscosities lower than 0.005 Pa.s no wave amplitude reduction was observed at highest Reynolds numbers achievable in UH experiments. For viscosities higher than 0.025 Pa.s, the maximum wave amplitude increased monotonically until the annular flow became slug flow. Increasing the Reynolds number after annular-slug transition did not reverse the type of the flow.

A new model is used to explain the experimentally observed phenomenon of wave suppression. The model predicts the suppression of waves and completely flat films at high Reynolds numbers.

Seven sets of experiments were conducted aboard the KC-135 aircraft to study the characteristics of wavy films in annular gas-liquid flows in the viscous regime to determine the slug-annular transition and pressure drop for circumstances in microgravity. The two-phase pressure drop and statistics of the wavy film were also determined as a function of gas and liquid Reynolds numbers and a preliminary analysis.

TWO-PHASE GAS-LIQUID AND VAPOR-LIQUID FLOWS OCCUR IN A variety of situations in chemical processing, power generation and energy production facilities. In addition to these normal gravity applications, such flows also occur in many space operations such as active thermal control systems, power cycles, propulsion devices, storage and transfer of cryogenic fluids, and recycling operations.

Two-phase flows can be grouped into a number of different flow patterns. These flow patterns are based on the spatial and temporal distribution of the vapor (or gas) and liquid phases. Gravity is a major reason for such two-phase flows to exhibit a wide range of flow patterns with different characteristics. The

gravitational body force acting on the phases with different densities causes stratification. In addition to the magnitude of that body force, orientation of body force with respect to the direction of flow has a strong impact on the flow patterns observed and also on the flow pattern transition boundaries. For example, normal gravity vertical upward co-current flow exhibits the following flow patterns: annular, churn, slug, and bubbly. On the other hand, normal gravity horizontal flow exhibits the following flow patterns: smooth stratified, wavy stratified, elongated bubble, dispersed bubble, plug, slug and annular.

Recent experiments have shown that two-phase flow patterns are somewhat simplified in microgravity. For example, only three major flow patterns (bubble, slug and annular) have been observed. In addition, annular flow is obtained for a wide range of gas and liquid flow rates in microgravity. It is the preferred flow pattern for the operation of two-phase systems in space. Slug flow is avoided, because vibrations caused by slugs result in unwanted accelerations. In many cases, bubbly flow should also be avoided because of the difficulty of preventing the transition from bubbly flow to slug flow. Therefore, it is important to be able to accurately predict the flow pattern that may exist under given operating conditions of a two-phase system.

Wavy liquid film in annular flow has a profound influence on the transfer of momentum and heat between the gas and the liquid. Thus, an understanding of the characteristics of the wavy film is essential for developing accurate correlations that may be used to predict the transfer rates. The main goal of our work is to understand through a combined program of experimental, and modeling studies, two-phase gas-liquid flows in pipes under normal as well as reduced gravity conditions.

A brief summary of our experimental and modeling studies in normal as well as microgravity conditions is given here.

Experimental and Modeling Studies on Wave Suppression on Vertically Falling Films

The main goal of our work on wavy films in vertical pipes is to determine the relationship between the maximum wave amplitude and the physical parameters, namely Reynolds, Kapitza, or Weber numbers, which characterize the system. The maximum wave amplitude in a free falling film depends only on the system parameters and is proven insensitive to external noise. More important, since the large waves dominate the transfer processes, one can expect the heat and mass transfer to be strongly correlated with the maximum wave amplitude.

Experiments were conducted using flow loops, which consist of three sections: the feed section, the flow development section, and the test measurement section. Time traces of film thickness were measured for two internal diameter flow loops using half inch and 0.75-inch vertical acrylic columns. All the flow characteristics such as the wave amplitude, shape, and wave speed reach steady states and can be observed in the test measurement section. The measurement section equipped with six conductance probes measures the electrical conductance between the twin platinum-rhodium parallel wires with the diameter 0.076 mm. The distance between the feed section and the probes is 2.65 meters and it is assumed that the flow is fully developed at the last probe.

In these experiments, researchers observed a new phenomenon of wave suppression at moderately high Reynolds numbers. The maximum as well as the average wave amplitudes reach a maximum value at some Reynolds number and then start to decrease.

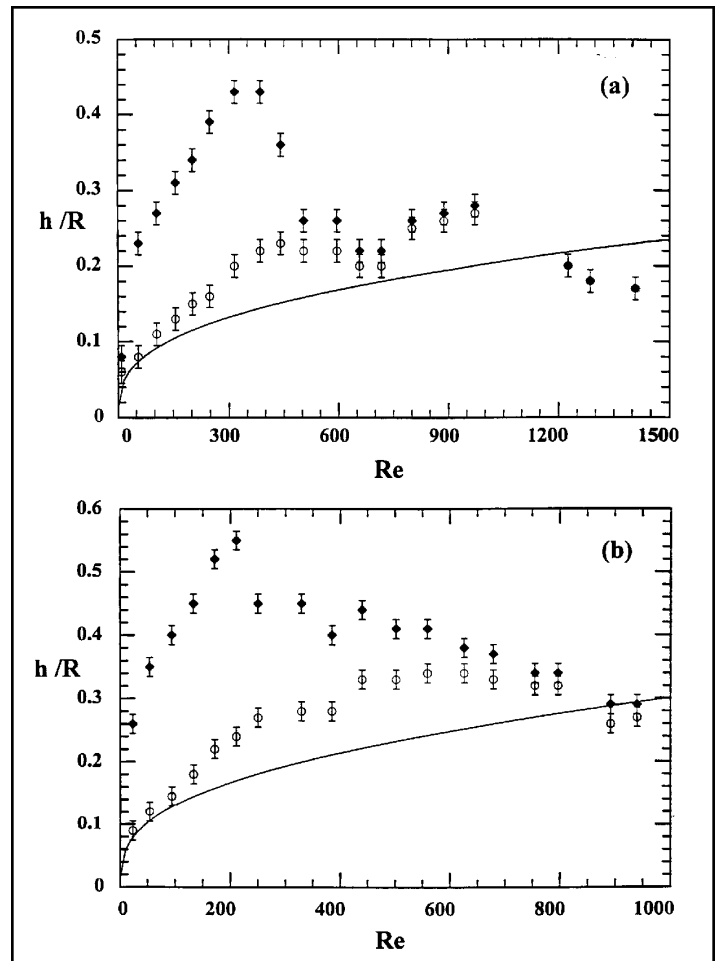


Figure 1. Maximum, average and Nusselt film thickness as a function of Reynolds Number: (a) viscosity 0.00525 Pa.s, (b) viscosity 0.00914 Pa.s. The solid line is a plot of the Nusselt film thickness.

The experimental data for 1/2 inch column are shown in Figs. 1,2 for viscosities 0.0033 Pa.s, 0.00525 Pa.s, 0.00914 Pa.s, 0.0115 Pa.s, where the maximum and the average film thickness are presented as a function of the Reynolds number. This observation is contrary to well-established point of view that wave amplitude increases with the Reynolds number. In these experiments, completely flat films were observed at high Reynolds numbers. One can see that after some Reynolds number the maximum and the average film thickness are almost identical. In the experiments, we observed flat films near the measurement section, while in the flow development section, the waves could be seen clearly. For higher viscosities 0.042.2 Pa.s, 0.0818 Pa.s, 0.656 Pa.s, the maximum wave amplitude increased monotonically until the annular flow became slug flow. For higher viscosity the annular-slug transition becomes sharper. We observed that transition takes place in a narrow interval of Reynolds numbers. Increasing the Reynolds number after annular-slug transition did not reverse the type of the flow.

Similar series of experiments were conducted in a 3/4-inch column. We observed that the maximum amplitude starts to decrease while the average amplitude reaches saturation. Unfortunately larger column diameter required larger volumetric flow at the same Reynolds number, so we could not reach higher

Investigative team

UH PI: Vemuri Balakotaiah, Ph.D., Professor
Department of Chemical Engineering
Cullen College of Engineering
University of Houston
Houston, TX 77204-4792
Phone: (713) 743-4318; Fax: (713) 743-4323
E-mail: bala@uh.edu

UH PDAF: Dmitri Lastochkin, Ph.D.
Department of Chemical Engineering
Cullen College of Engineering
University of Houston
Houston, TX 77204-4792
Phone: (713) 743-4338; Fax: (713) 743-4323
E-mail: dmitri@uh.edu

NASA-JSC PI: Eugene Ungar, Ph.D.
Crew and Thermal Systems
Code EC2
NASA Johnson Space Center
2101 NASA Road 1
Houston, TX 77058
Phone: (713) 483-9115
E-mail: eungar@ems.jsc.nasa.gov

NASA-GRC PI: Brian J. Motil
Microgravity Science Division
NASA Glenn Research Center
21000 Brookpark Road, MS 500-102
Cleveland, OH 44135
Phone: (216) 433-6617
Lab: (216) 433-3971; Fax: (216) 433-8050
E-mail: brian.motil@grc.nasa.gov

Graduate Students:
Eric K. Dao, Ph.D. (Dec. 2001)
Department of Chemical Engineering
University of Houston
Houston, TX 77204-4792
E-mail: kdao2@bayou.uh.edu

Mohan Panga
Department of Chemical Engineering
University of Houston
Houston, TX 77204-4792
E-mail: panga_mohan@hotmail.com

Ramesh Mudunuri, doctoral student, will be continuing this work from May of 2002

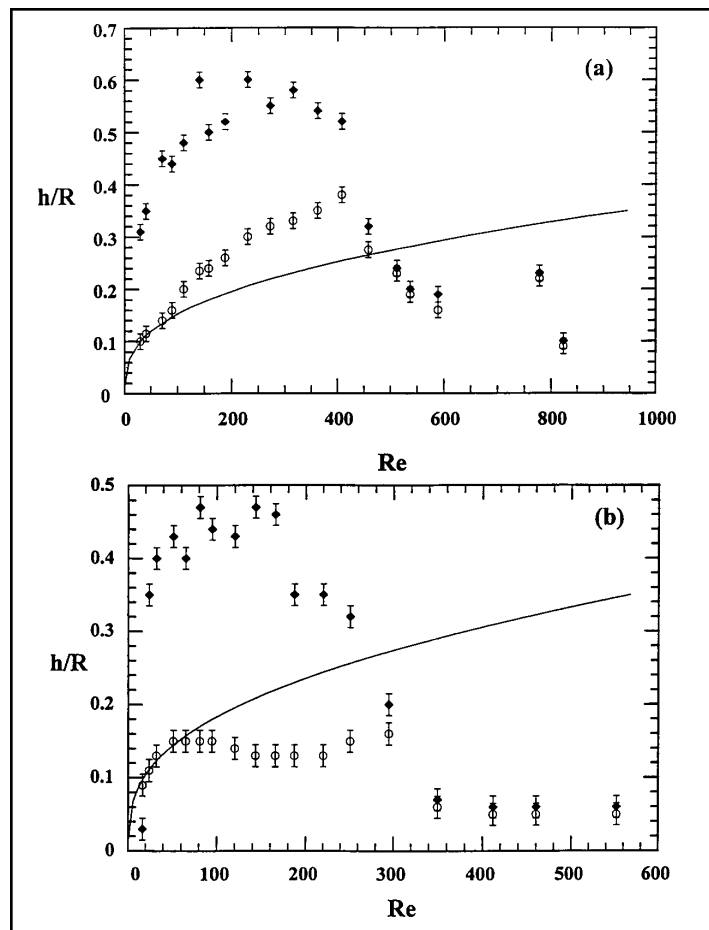


Figure 2. Maximum, average and Nusselt film thickness as a function of Reynolds Number: (a) viscosity 0.00115 Pa.s, (b) viscosity 0.00151 Pa.s. The solid line is a plot of the Nusselt film thickness.

Reynolds to see the effect more clearly. Slug-annular transition on 3/4-inch column takes place at higher viscosity and not so sharp as in the case of 1/2-inch column.

A new model was developed to predict the experimentally observed phenomenon of completely flat films for high Reynolds numbers. This model is an extension of that developed by Nguyen and Balakotaiah.¹ The model predicts the Reynolds number at which the wave amplitude starts to decrease. However, the model predicts lower maximum amplitude than the experimental value. The reasons for this can be explained: first-the model was derived under the assumption of flat geometry and does not take into consideration the tube curvature into consideration. It is well known that the tube curvature increases the wave amplitude especially for viscous fluids when liquid film occupies a large fraction of tube volume. Second, the model assumes traveling wave transformation which limitation, by its nature, cannot predict coalescence of waves, which can lead to the formation of a big wave. Taking these two factors into consideration, we can conclude that the theoretically predicted maximum amplitude must be lower than the experimentally observed values. (See Fig. 3).

Slug-Annular Transition in Microgravity

We have also conducted experiments on gas-liquid two-phase flows by using the KC-135 aircraft (of NASA-JSC) which, in parabolic trajectories, gives about 20 seconds of microgravity. The

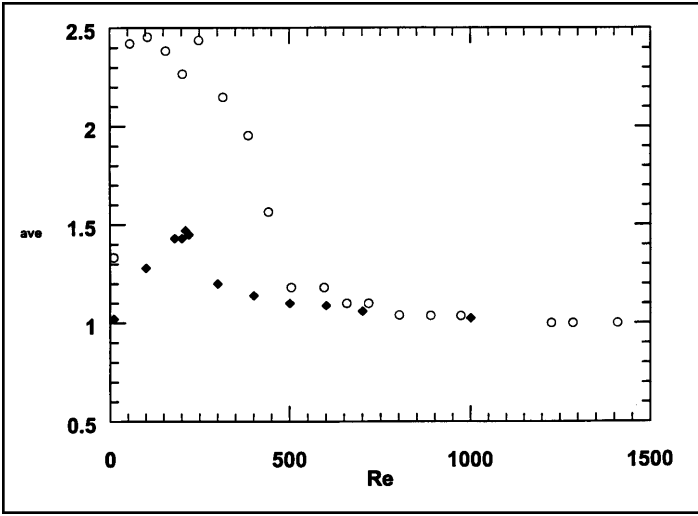


Figure 3 Comparison of experimental and theoretical ratio of maximum to average amplitude, viscosity 0.00525 Pa.s.

purpose of these experiments is to extend and verify the the flow pattern map developed recently by Jayawardena et al.² as well as to measure the pressure drop and wave amplitudes in annular flow.

As discussed elsewhere in detail,² the flow pattern in microgravity depends on eight variables (ρ_G , μ_G , ρ_L , μ_L , u_{LS} , u_{GS} , σ , and D). From these eight variables five dimensionless groups can be formed, the liquid Reynolds number, $Re_{LS} = \rho_L u_{LS} D / \mu_L$, the gas Reynolds number, $Re_{GS} = \rho_G u_{GS} D / \mu_G$, the viscosity ratio, μ_G / μ_L , the density ratio, ρ_G / ρ_L , and the Suratman number, $Su = \rho_L D \sigma / \mu_L^2$. Here, u_{LS} and u_{GS} denote the superficial velocity of liquid and gas based on single-phase flow, where D is the tube diameter, ρ , μ , and σ are density, viscosity, and surface tension respectively. The subscripts Land G denote liquid and gas phase. We assumed that the density and viscosity ratios have little effect on the transition boundary and the flow characteristics. Other possible dimensionless groups can replace the Suratman number such as

- The Weber number, $We = \frac{\rho_L u_{LS}^2 D}{\sigma}$,
- The Capillary number, $Ca = \frac{We_L}{Re_L} = \frac{Re_L}{Su} = \frac{\mu_L u_{LS}}{\sigma}$,
- The Ohnesorge number, $Oh = \frac{1}{Su}^{1/2} = \frac{\mu_L}{(\sigma D \rho_L)^{1/2}}$

Thus, we can express the critical liquid flow rate at slug-annular transition (Re_{LS}) as a function of the other two dimensionless groups, i.e. the gas flow rate (Re_{GS}) and the Suratman number. The slug-annular transition for microgravity two-phase viscous flows is shown in Fig. 4. The plot shows the dependence of the Reynolds ratio at the transition on the Suratman number of power $-3/2$, which is consistent with the results known in literature. It shows that the transition boundary determined by Jayawardena et al.² extends to much lower values of the Suratman number (viscous regime).

Pressure Drop in Two-Phase Flows in Microgravity

The pressure drop encountered in an annular flow system is one

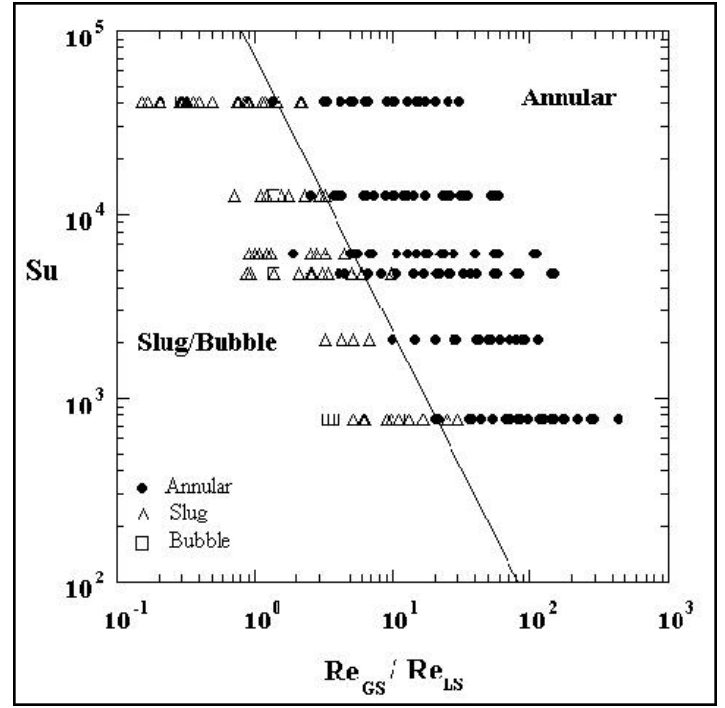


Figure 4. Flow pattern map for slug-annular transition in microgravity two-phase flow.

of the most important parameters to the designers of these systems. We do not attempt to test the homogeneous model with our bubbly and slug pressure measurements, but rather focus on comparing the separated Lockhart-Martinelli flow model with pressure drop data in annular flows. By introducing a thin liquid film onto the inside perimeter of the gas pipe, the pressure drop can be increased by an order of magnitude. For annular flows, the separated model is more appropriate than homogeneous models because of considerable slip between the phases. One of the most time-tested annular pressure drop models is the Lockhart-Martinelli model. In this model, the pressure drop of annular two-phase flow is related to the pressure drops of each phase flowing alone in the pipe. Since the correlations for single-phase pressure drop are well established, the Lockhart-Martinelli model has the advantage of being easy to use. In the Lockhart-Martinelli model, the gas two-phase flow multiplier $\frac{2}{G}$ is defined as

$$\frac{2}{G} = \frac{P_{TP}}{P_G}, \quad (1)$$

where P_{TP} is the two-phase pressure drop, and P_G is the gas pressure drop. The Lockhart-Martinelli model provides correlations for the multiplier based on the Martinelli parameter defined as

$$X^2 = \frac{P_L}{P_G}, \quad (2)$$

where P_L is the pressure drop of the liquid flowing alone in the tube. The original correlations consist of a set of graphs to predict the gas multiplier based on the gas/liquid phases laminar or turbulent.

$$\frac{2}{G} = 1 + C X + X^2, \quad (3) \quad \text{ISSO-13}$$

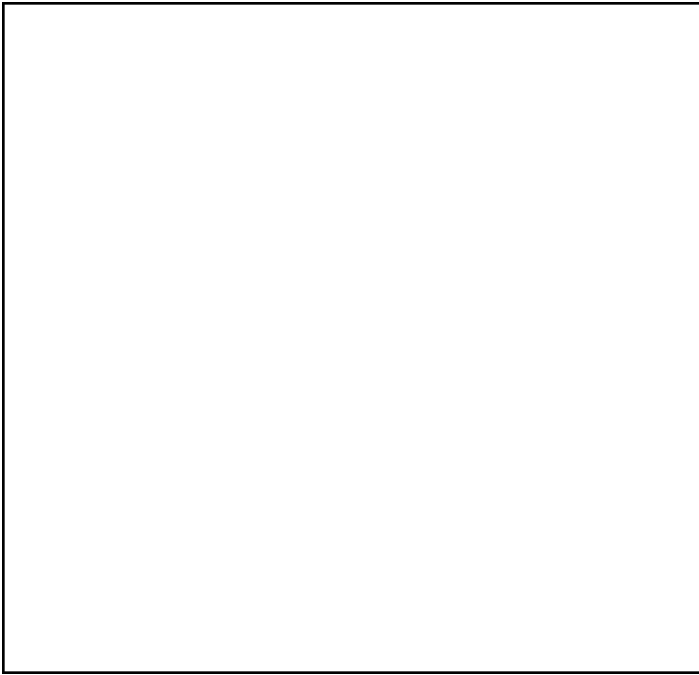


Figure 5. Experimental measured pressure drop in microgravity annular flow and prediction for three different liquid glycerin solutions.

where the value of C depends on the single-phase flow regimes (laminar or turbulent) of gas/liquid. The Martinelli parameter X can be calculated from the single-phase pressure drops (Eq. 2), using the standard friction factor approach. The Fanning equation for single-phase pressure drop is defined as

$$-\frac{dP}{dx} = \frac{2 f \rho u^2}{D} \quad (4)$$

The friction factor is defined as

$$f = \frac{C_B}{Re^n}, \quad (5)$$

where $C_B = 16$, $n = 1$ for laminar flow ($Re < 2000$) and $C_B = 0.046$, and $n = 0.2$ for turbulent flow ($Re > 2000$). When the values of X and C_G are determined, the two-phase pressure drop is calculated from Equation (2).

We used the Lockhart-Martinelli model to predict the pressure drop and compare with the measured pressure drop in microgravity annular flow. The single-phase pressure gradients are calculated with the friction factors, $f = 16/Re$ for $Re < 2000$, and $f = 0.0791 / Re^{1/4}$ for $Re > 2000$. For annular flow in half-inch diameter tube, we used the same Equation (3) for the gas multiplier and found the constant C to be 18 for turbulent gas and laminar liquid flows

$$\frac{2}{G} = 1 + 18 X + X^2. \quad (6)$$

Figure 5 shows the comparison between the measured pressure drops and the predictions using Eq. (6). Points on the 45-degree line indicate the exact match between measured and predicted values. The pressure drops predicted by L-M corre-

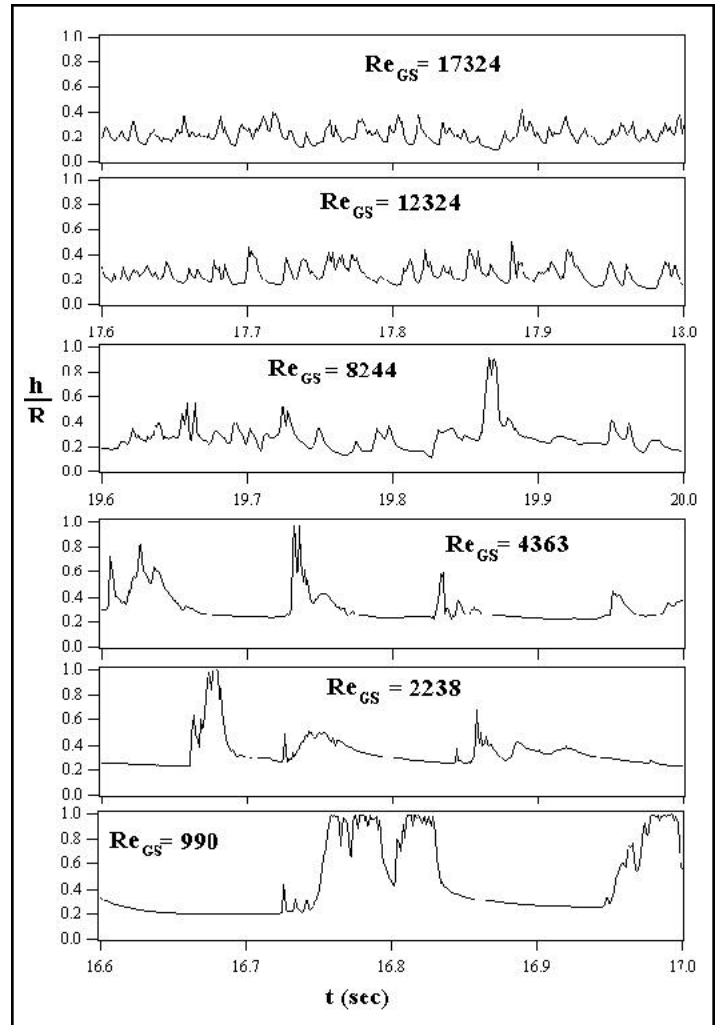


Figure 6. Film thickness traces collected at probe # 6 ($Su = 768.8$) at fixed $Re_{LS} = 100$.

lation with Equation (6) give good agreement with the measured pressure drops for annular flow with turbulent gas and laminar liquid flowing ranges.

Wave Characteristics

Conductance probe data allow for additional analysis of the characteristics of annular waves beyond the qualitative results presented previously. By using six conductance probes located six inches apart, we can study the behavior of each particular wave as it traveled through the test tube. This may lead to a better understanding of the processes occurring in and around the annular waves in microgravity. In the experiment, we fixed the liquid flow rate and reduced the gas flow rate until wave occlusion occurred. Figure 6 shows the film thickness collected at probe no. 6 for fixed liquid flow rate ($Re_{LS} \sim 100$, $Su = 768.8$). The film thickness increases as we reduce the gas flow rate from $Re_{GS} = 17324$ to 4363. At $Re_{GS} = 2238$ wave occlusion occurs and annular flow becomes slug flow. Figure 7 shows the experimental scaled film thickness as a function of the Reynolds ratio (Re_{LS}/Re_{GS}) for a liquid Suratman number of 12624.7. The film thickness is chosen to be the average value of the film thickness collected at probe no. 5 and Probe no. 6. Figure 8 presents the plot of the scaled film thickness versus the Reynolds ratio with fixed liquid Reynolds numbers at 56, 100 and 110 ($Su = 768.8$). As we reduce the gas

